Oxide phases induced by electron irradiation at model pwrs 316l /water interfaces at high temperature and pression

M. Wang, C. Corbel, S. Perrin, D. Feron

Oxydes formés à haute température et pression par irradiation aux électrons d'interfaces 316L/Eau(REP)

Laboratoire des Solides Irradiés, UMR 7642
M. Wang Ph-D (2010-2013), C. Corbel

SCCME/Laboratoire d'Etudes de Corrosion Aqueuse
S. Perrin, D. Féron

Conditions Extrêmes et Matériaux : Haute Température et Irradiation, UPR3079 CNRS
D. Simon

Réacteur à Eau Pressurisée
refroidissement du cœur
Circuit primaire sous flux neutrons, gammas

Matériau de Structure(irradiation)/Eau de Refroidissement(radiolyse)

Stabilité des composants

Corrosion sous irradiation

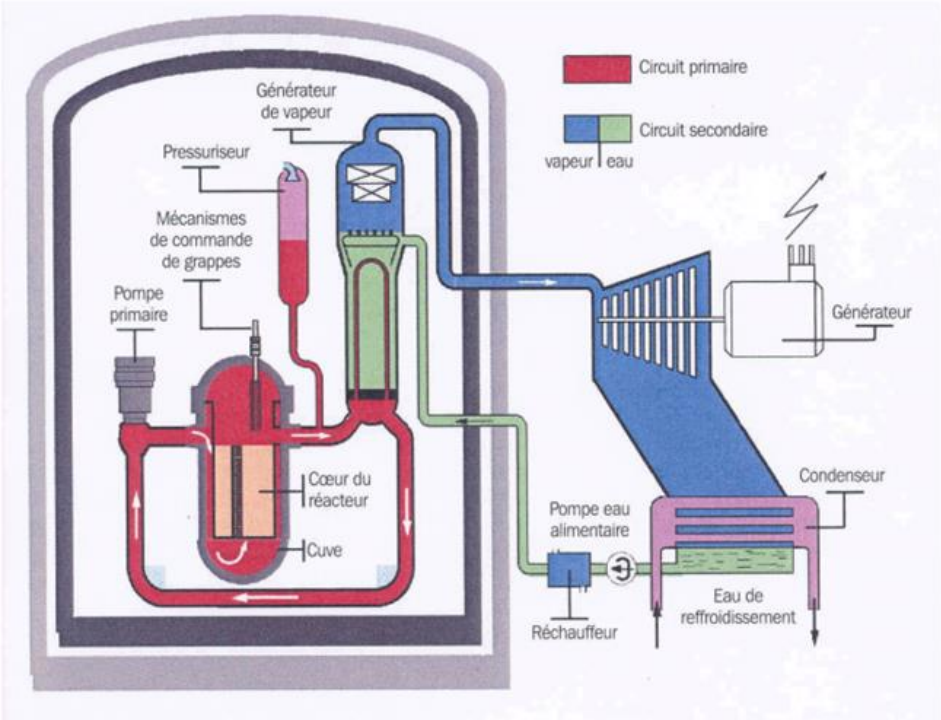

Croissance et Electrochimie

Oxyde hors ou sous Flux (H+ or e-)

[Temperature,Pressure](eau liq/vap)

[25°C, 0.1 MPa] - [300°C, 9 MPa]

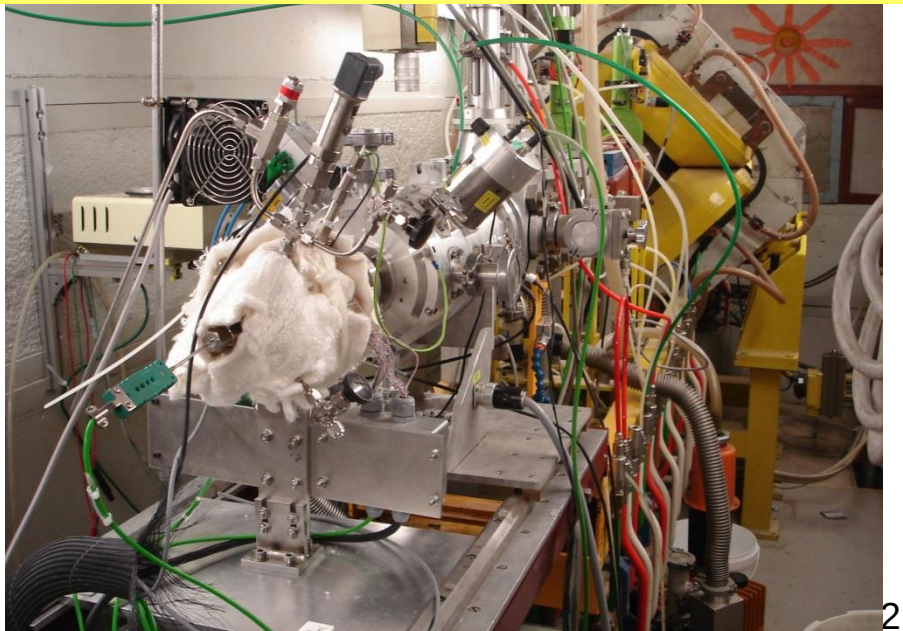

Corrosion under Irradiation: 316L-$Ox_{300°C}$ in PWR conditions

Primary coolant circuit

PWR Feed Water $H_2O(Li,B,H_2)$
$[H_{2aq}]$(cc(STP)/kg): 25-50

Interface 316L-$Ox_{300°C}/H_2O(Li,B,H_2)$

HTHP: ~300°C, ~155 bars, Flow rate, Flux(neutrons,gammas)=>(ions, protons, electrons)

316L-$Oxide_{300°C}$ Stability in ~300°C,~155 bar, flux

Stress-Microstructure(irradiation)-Chemical environment(radiolysis)

Free potential passive range

Long time for crack initiation and incubation

Low growth rate $(mm.s^{-1})<\sim 2x10^{-8}$

Reference 316L-$Oxide_{300°C}$ Stability in ~300°C, ~155 bars, no flux

Free potential E (V/SHE)<~(-0.23)

P.L. Andresen et al. JOM 1996, TMS 2005,Corrosion 64,2008

Failures in PWRs flux- Irradiation induced Stress Corrosion Cracking

In-pile Electrochemistry: 304L-$Ox_{300°C}$ in PWR conditions

PWR Feed Water $[H_{2aq}]$(cc(STP)/kg): 25-50
300°C,Thermal Neutron Flux($ncm^{-2}s^{-1}$)~1^E14

Molander et al. (Studvik) 1986, 1990 - Ringhals 4 PWR (Sweden)
Bosh et al. (SCK-CEN) JNM 2007- BR2-MRT PWR (Belgium)

Free Potential for S. Steels (304)

E(time,300°C)-SHE: cst for flux off or on

~-0.780 V/SHE at 300°C for H_2: 28(8) cc(STP) /kg [Bosh JNM 2007]

Vankeerberghen et al. (SCK-CEN) JNM 2003, Bosh et al.(SCK-CEN)) JNM 2007; Elec. Acta BR2-MRT PWR (Belgium)

Impedance for S. Steels (304)

304-Ox300°C/PWR(H_2) in-pile

300°C Thermal Neutron Flux($ncm^{-2}s^{-1}$)~1^E14

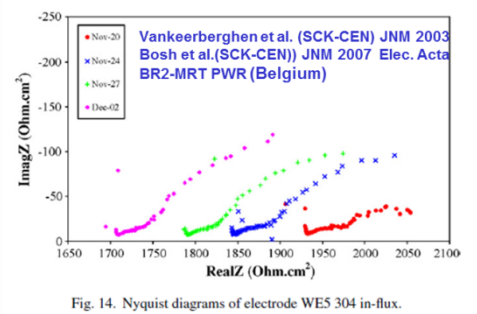

Fig. 14. Nyquist diagrams of electrode WE5 304 in-flux.

300°C Thermal Neutron Flux($ncm^{-2}s^{-1}$) ~0

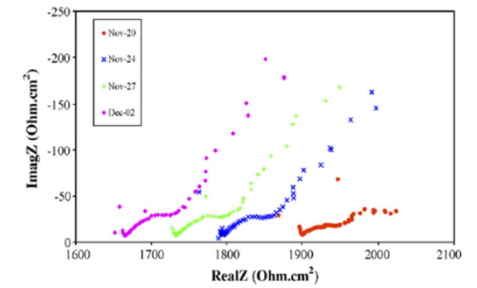

Fig. 13. Nyquist diagrams of electrode WE5 304 out-of-flux.

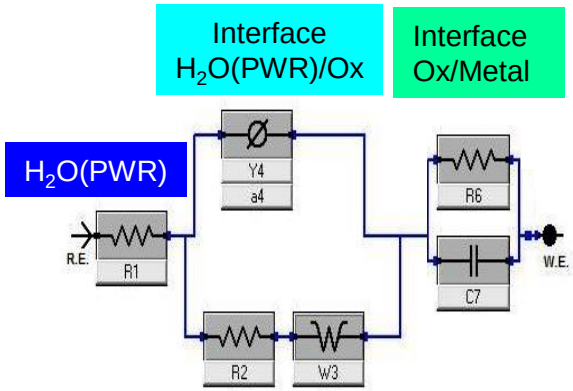

Z(time,300°C)
In-flux≠Out-of-flux
Small Difference

Ox thickness
Variability

In-flux: x10
Out-of-flux: x2

316L exposure to 300°C,90bar PWR chemistry without irradiation

In Situ Temperature &(Pressure)
Heating-300°C(7days)-Cooling

Pd/Ag Permeation Probe

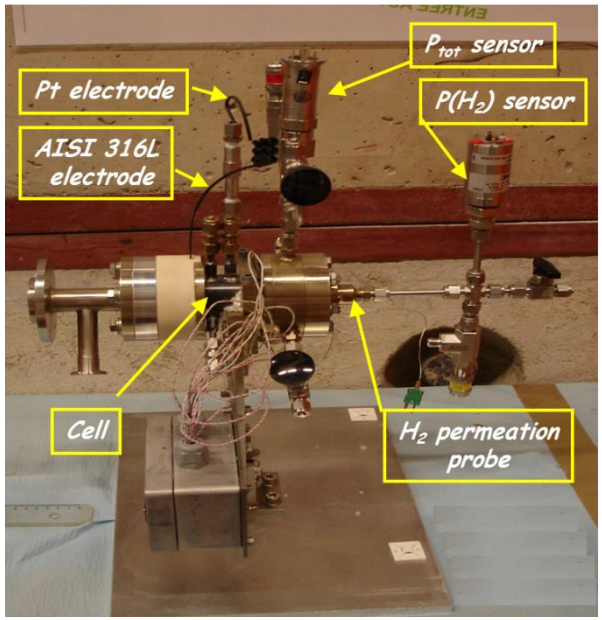

In Situ pH_2gas/cH_2aq*
* Permeation probe ≥200°C

pH_2gas/mbar (time,300°C):
6 to 60
x10

Pseudo Reference Electrode
Pt wire ($[H_2]/[O_2]$ >>8)

In Situ
Free Potential
316L vs Pt

Working Electrode
AISI 316L Disc

E_{316L} vs Pt/V(time,300°C)
Tup ΔE_{316L} <0; Tdn ΔE_{316L} >0

No flow rate

300°C:-0.039;min-0.096;-0.035

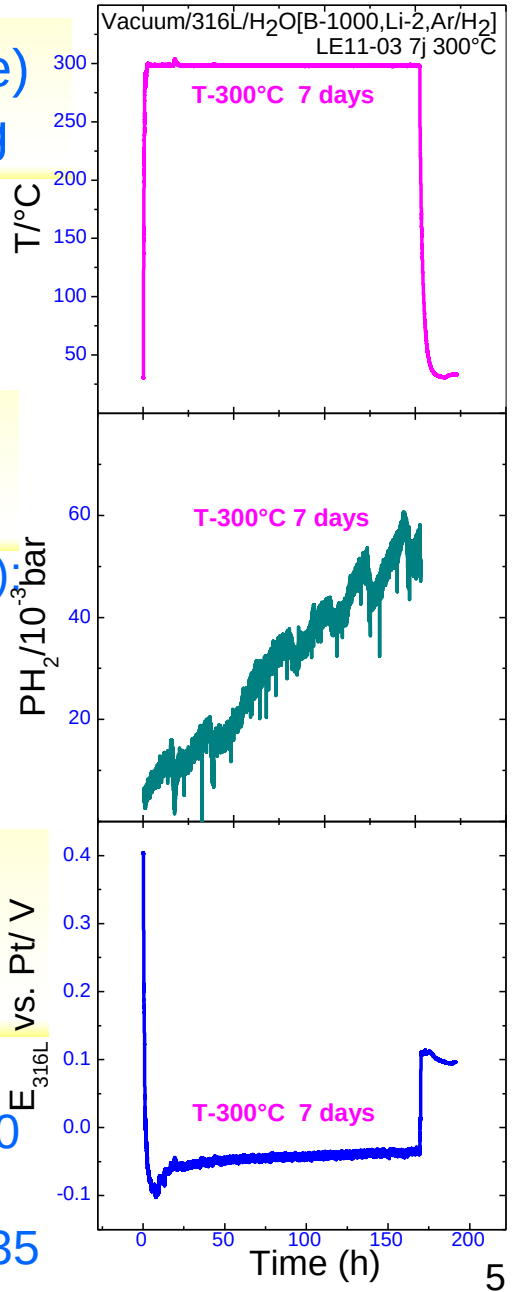

Disc(316L)/Water(PWR, Ar/x%H_2) Interface Irradiation [~300°C,~90bar]

Pd/Ag Permeation Probe

e- Pelletron SIRIUS-LSI

In-Line Beam Mounting

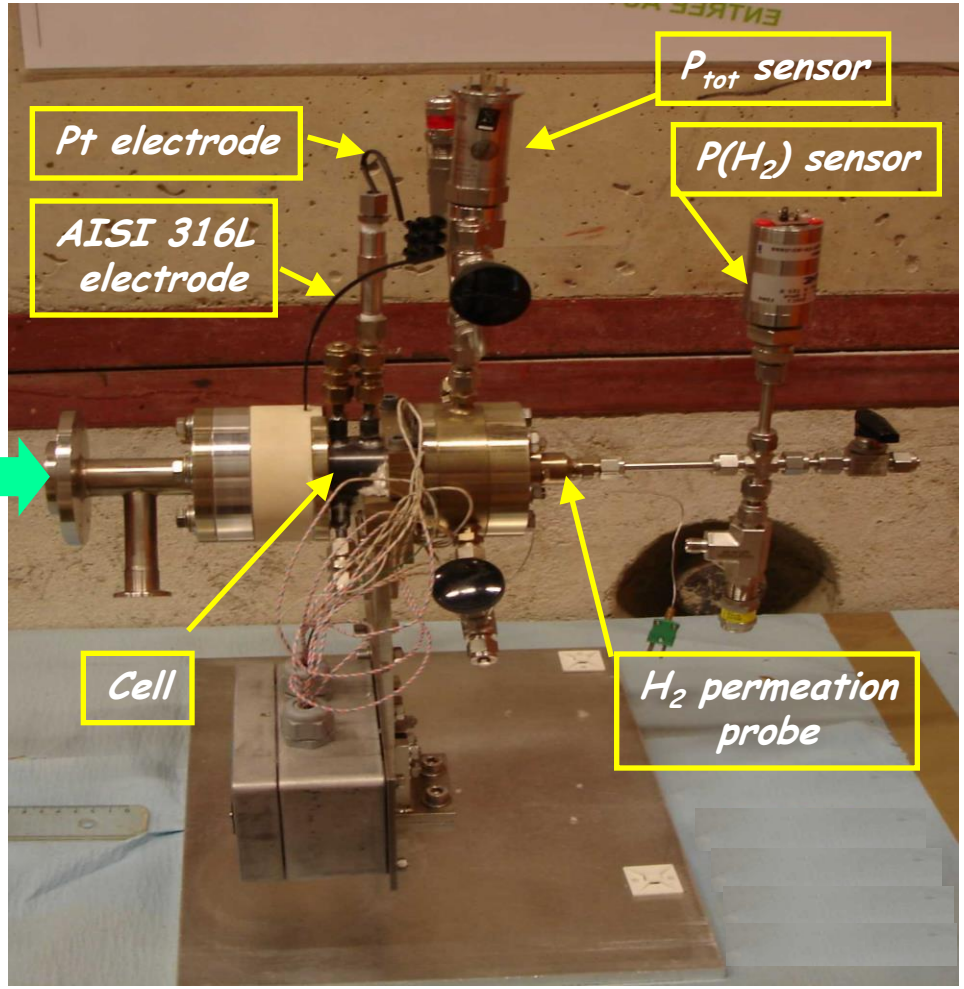

H+ cyclotron CEMHTI

Vacuum[flux]/Disc(316L)/Water(PWR, Ar/x%H_2)[flux;no flux]/Pt

316L exposure to 300°C,90bar PWR chemistry during e- irradiation

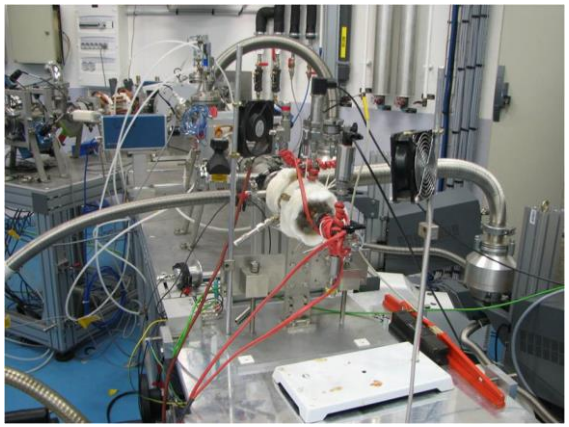

Pre-Irradiation Test 5 min, 25°C
Flux($e^-cm^{-2}s^{-1}$)≤ $2.02x10^{13}$

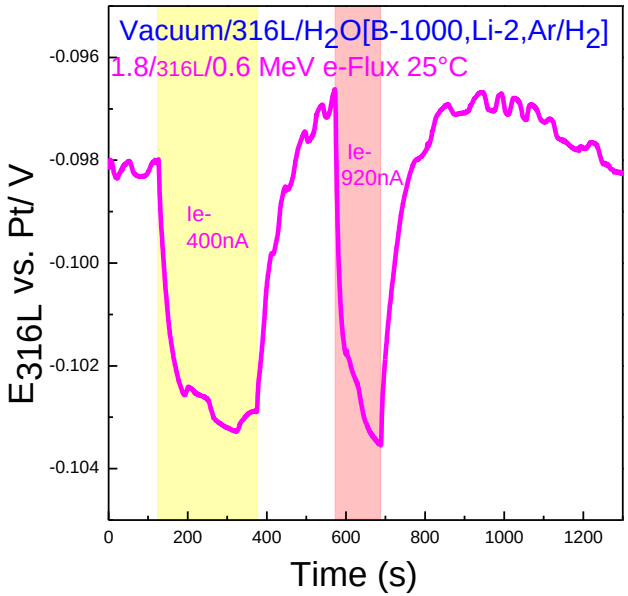

25°C e- Flux
on: $\Delta E_{316L}<0$; off: $\Delta E_{316L}>0$

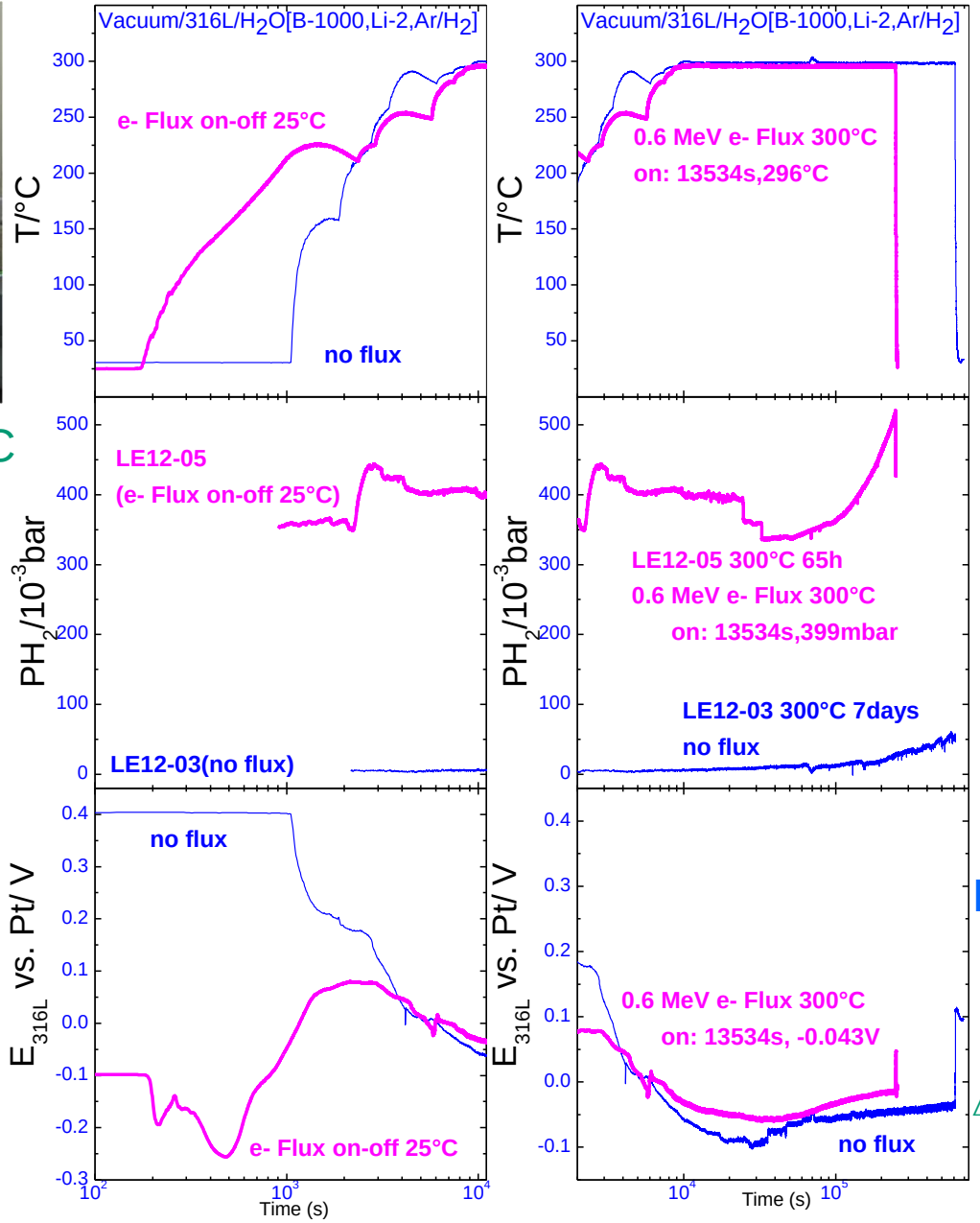

300°C
316L/PWR
0.6MeV e-
65h
Fluence
/(e^-cm^{-2})
≤ $4.7x10^{18}$

pH_2gaz
/mbar
Initial;final
399; 507
x1.27

E_{316L} vs Pt
/V
Initial;final
-0.043;-0.015
ΔE_{316}=0.028
$\Delta E_{316L}>0$

316L after 300°C,90bar exposure to PWR chemistry

Structural & Chemical Analysis (TEM M. Sennour Mines Paris Tech)

Microstructure

Surface: SEM (Scanning Electron Microscope)

Depth Profiling: TEM (Transmission Electron Microscope) cross section

Crystalline structure

Depth Profiling: SAD (selected aera diffraction) -TEM

Phase composition

Depth Profiling: HAADF (high angle annular dark field) -STEM &

EDX (energy dispersive X-ray spectroscopy)

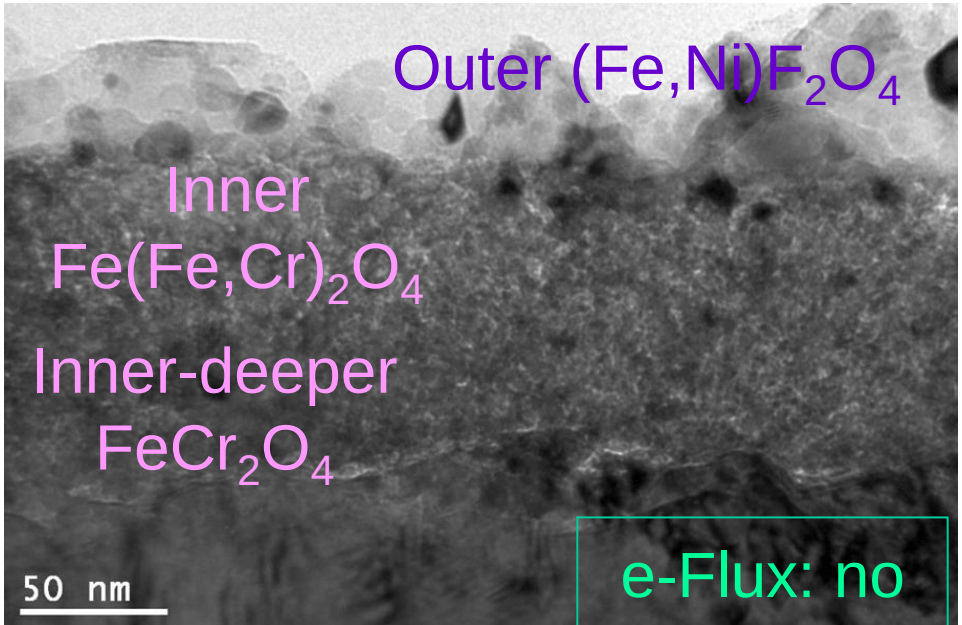

LE11-02 no flux

300°C, 72 hrs,pH_2/mbar: 133-166

Bi-layer oxide

heterogeneous thickness

Inner: chromite, Fe(III)-rich chromite

Outer: crystallites Fe(II)-rich trevorite

Consistent with literature

e.g. Takumi TERACHI et al. 2008 J.Nuclear Science and Technology, 45:10, 975-984

316L bulk & bi-layered surface oxide after e-Irradiation at HTHP,(~(300°C,90 bar))

Synthesis of Structural & Chemical Analysis

Depth~(>0.1-04 µm) – Bulk

Strong texture
high defect density
(dislocations lines or loops, stacking faults, black dots, no cavity)

Depth~(0.1-0.4 µm) – Bulk/ Inner oxide boundary

Oxide Growth: effect of the texture
Boundary (saw tooth directions) in relation with texture

Depth~(< 0.1-0.4 µm) – Oxide layer

Inner-layer (dense) : Fe(III)-enriched nickel chromite, $Ni(Fe,Cr)_2O_4$

outer-layer (dispersed crystallites (<50nm)): Fe(III) hematite α-Fe_2O_3

Inner-layer destruction: low density distribution of cavity (~(0.2-5) μm^2, depth (1-1.5µm), ~(1-5)x10^{-9} cm^{-2}

Microstructure after e- Irradiation at ~300°C,90bar

316L Disc Surface (PWR Face)–SEM

~80x60µm2 (left) & ~8x6µm2 (right)

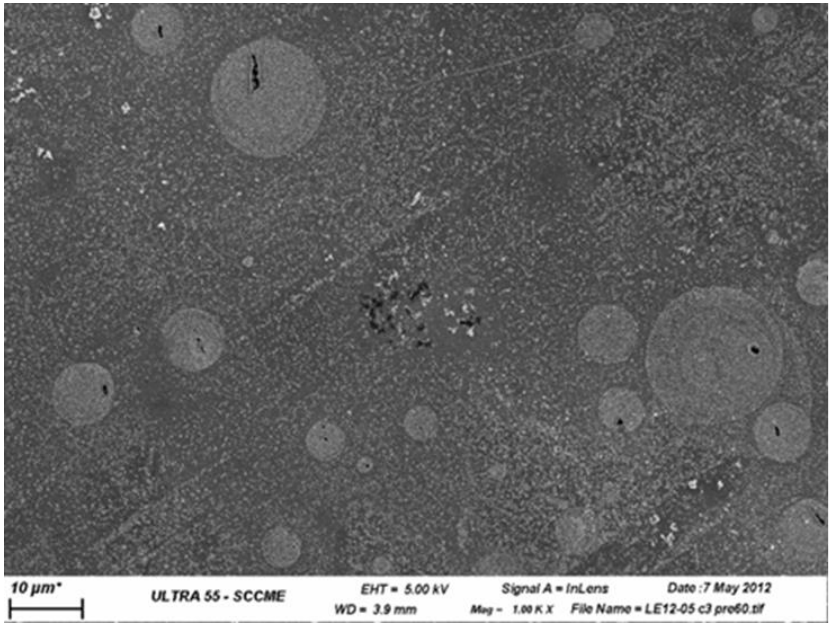

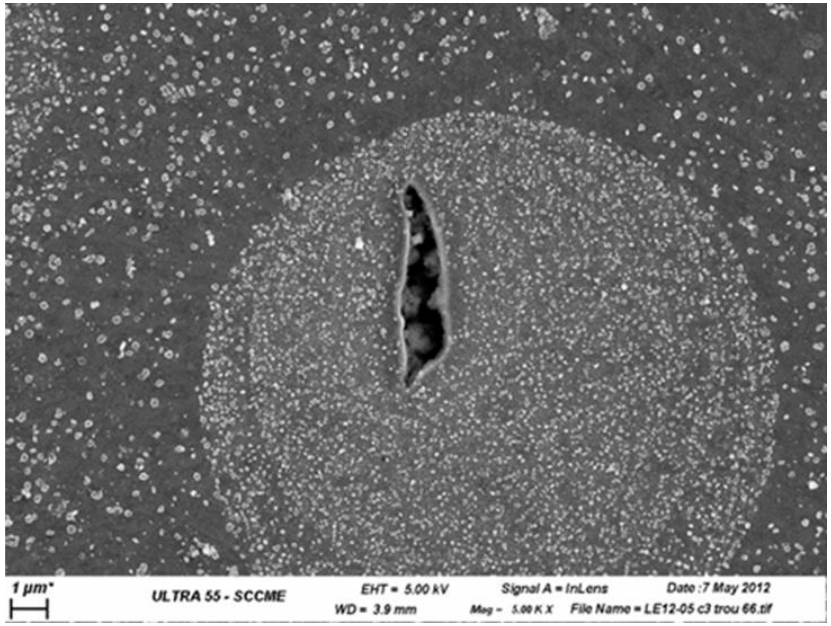

Image: strong contrast variation
Inhomogeneous surface
Random distribution:

White parallel lines
White discs 2r(1-20µm)
Black spots L(<6µm)
White tiny dots(<<0.1 µm)

Microstructure after e- Irradiation at ~300°C,90bar

316L Disc Surface (PWR Face)–SEM

SEM images (~5x3µm2)

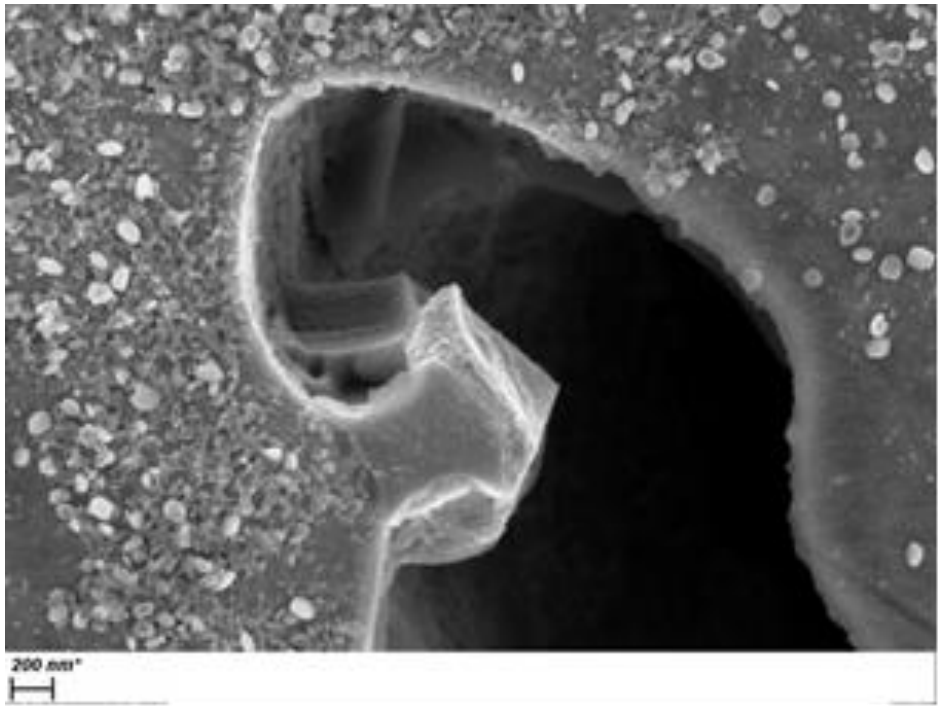

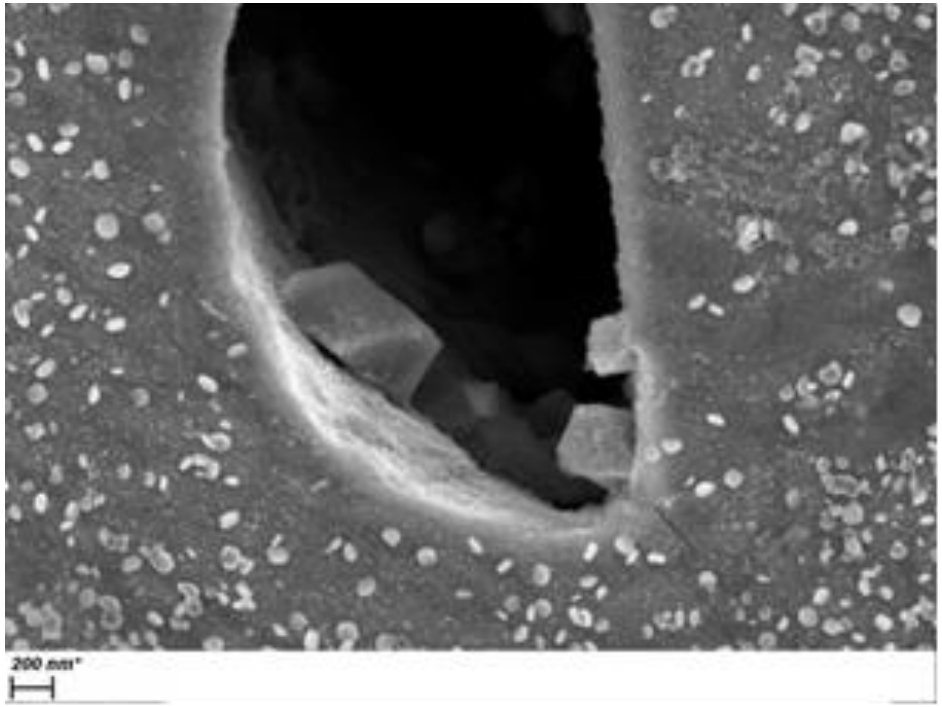

Cavities (black spots):

Cross-section at surface ~(0.2-5µm^2)

Depth penetration (interferometry profile) ~(1-1.5µm)

Wall decoration with tiny fragments

Edge with fracture

Depth Profile of Microstructure after e- Irradiation at ~300°C,90 bar

316L Disc Depth profiling (PWR Face)–TEM

TEM cross-section image (~6x6 µm2)

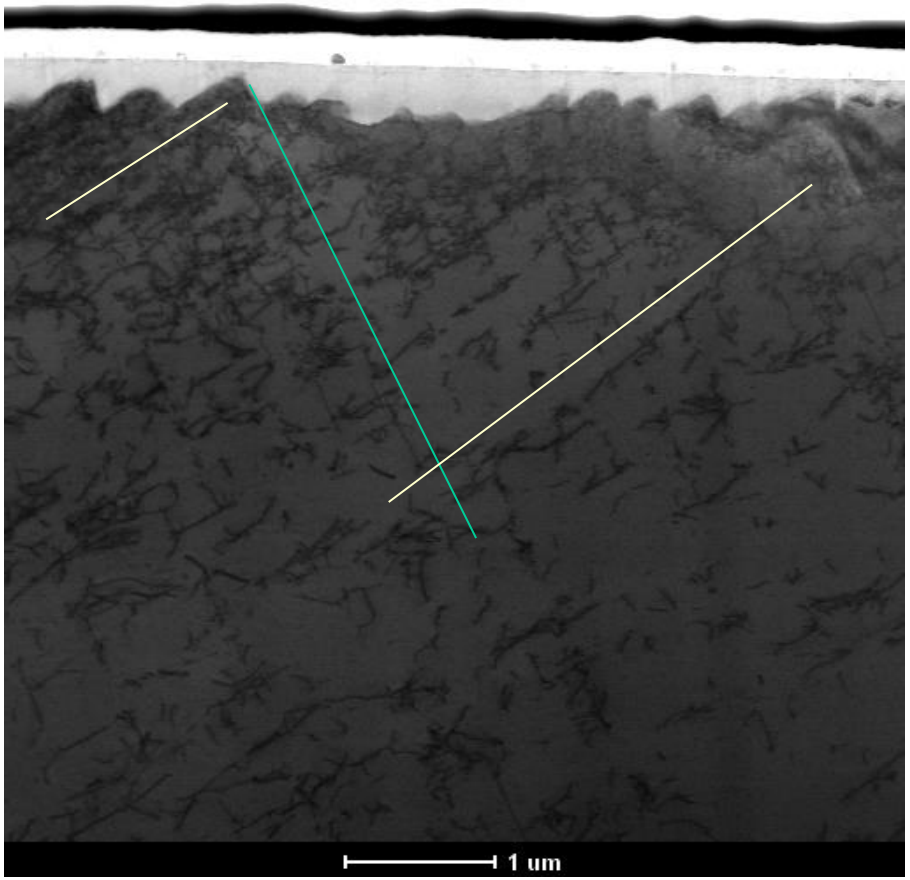

Depth~(<0.4 µm) – Bulk

Alignment of black segments: two preferential directions

Depth~(0.1-0.4 µm) – Bulk/ Surface layer limit

Saw Tooth pattern of boundary (edge // black segments)

Depth Profile of Microstructure after e- Irradiation at ~300°C,90 bar

316L Disc Depth profiling (PWR Face)–TEM

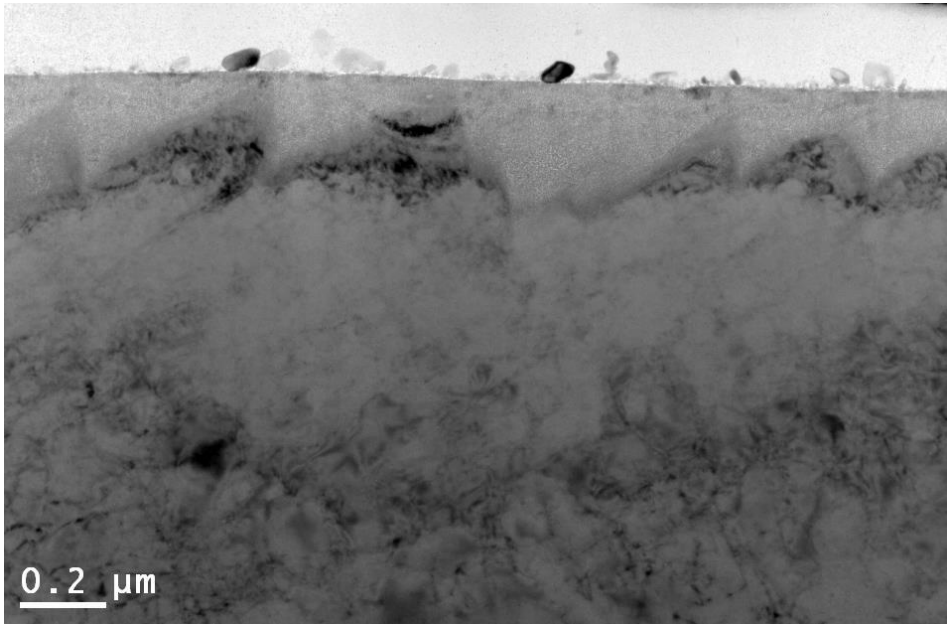

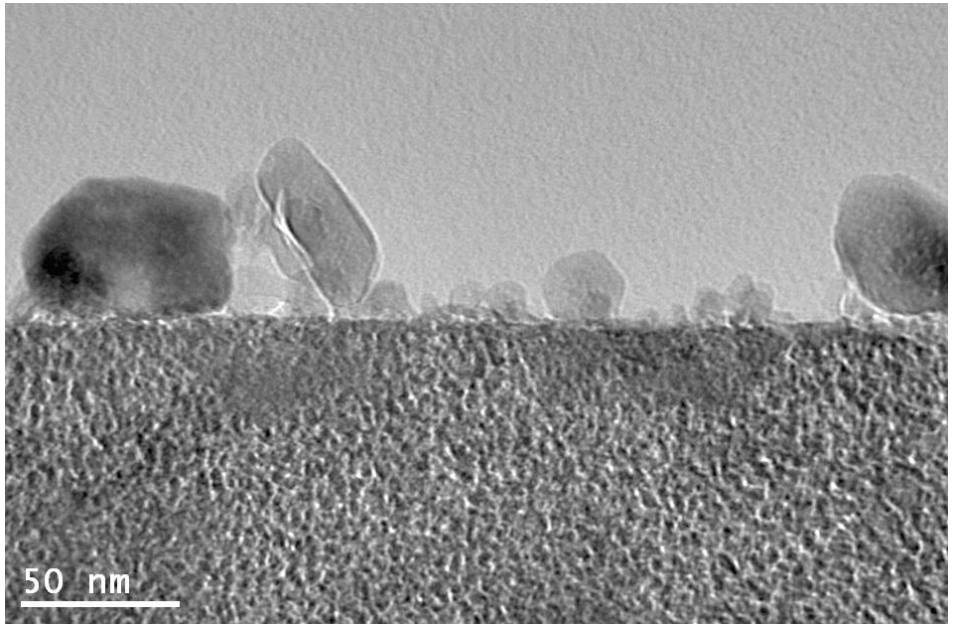

Depth~(<0.1-0.4 µm) – Near Surface

Double layer structure

Inner layer structure (below surface)

Disc-like nano-grains 2r~(3nm)

Saw Tooth boundary (variable thickness)

Outer layer structure (top flat surface)

Distribution of tiny fragments ~L(5-50 nm)

Crystalline Structure after ~300°C,90bar e- Irradiation

Cross view: Selected Area Diffraction TEM
Bulk & Bulk/Surface layer limit (red circle)

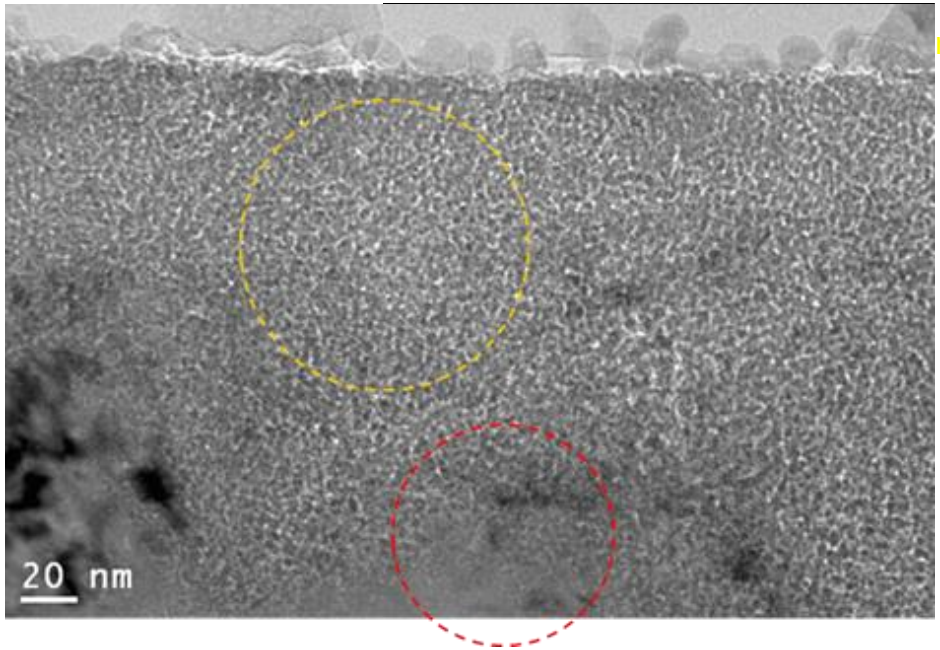

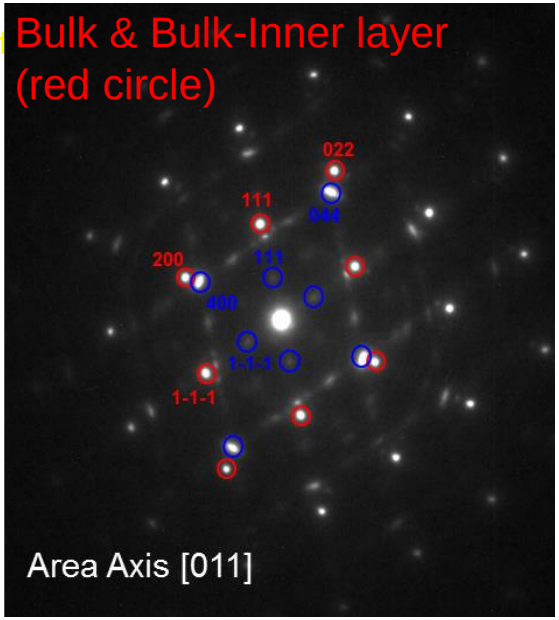

Depth~(<0.4 µm) – Bulk

Polycrystalline; Cubic; Face Centered lattice;316L austenitic steel

Depth~(0.1-0.4 µm) – Bulk/ Surface layer limit

Correspondence between the Indexing of diffraction peaks: growth of surface layer in epitaxy with bulk

Crystalline Structure after ~300°C,90bar e- Irradiation

Cross view: Selected Area Diffraction TEM

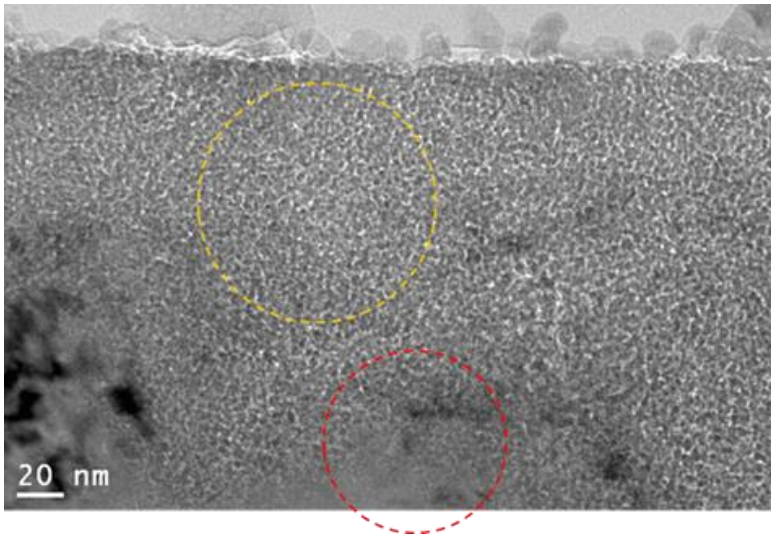

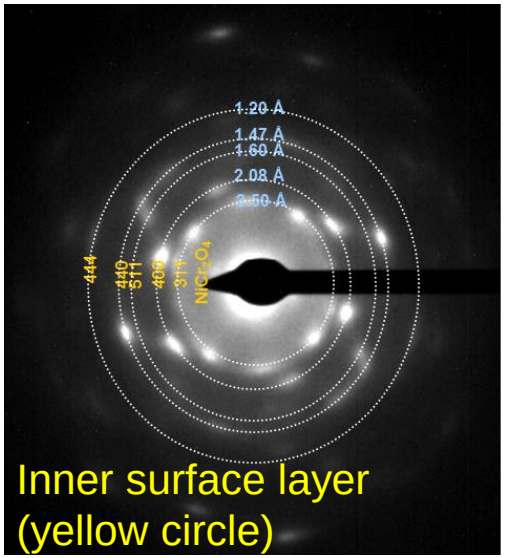

Depth~(<0.-0.4 μm) – Near Surface

Double layer structure

Inner layer structure (below surface)

Polycrystalline; Cubic; spinel-type lattice; $NiCr_2O_4$ nickel chromite

Crystalline Structure after ~300°C,90bar e- Irradiation

Cross view: Selected Area Diffraction TEM
Outer Surface Layer (red circle)

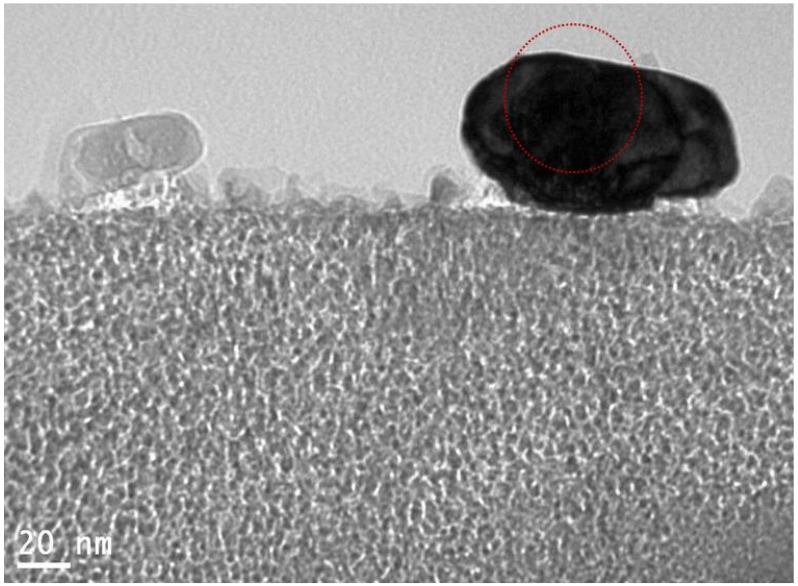

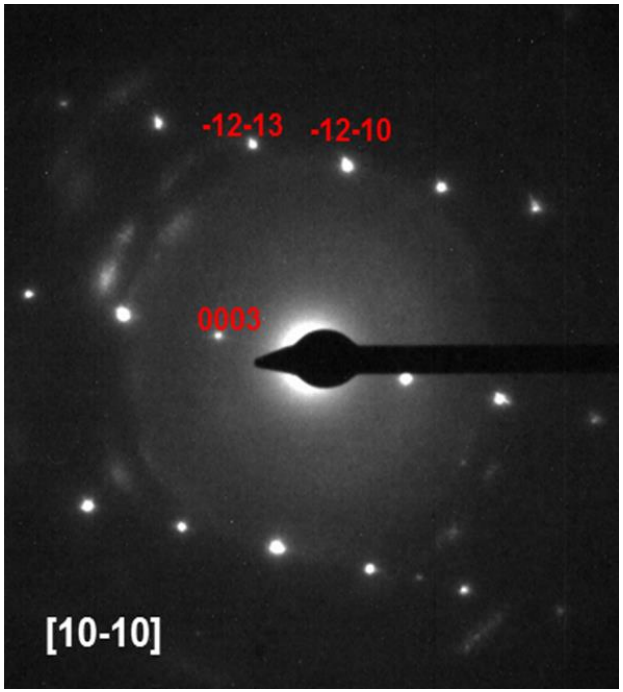

Depth~(<0.-0.4 µm) – Near Surface

Double layer structure

Outer layer structure (top flat surface)

Distribution of tiny crystallites ~L(5-50 nm)

Single crystal; Trigonal; corundum-type lattice; α-Fe_2O_3 hematite

High-resolution transmission electron microscopy (HRTEM) images (cross –sectional view) and their corresponding Fourier Transform (FT) diffractograms were also recorded inside and at the periphery of some surface crystallites: analysis consistent with single crystal hematite.

Oxide Growth on 316L at ~(300°C,90 bar): e- flux effect Synthesis of Structural & Chemical Analysis

[cH_2](Initial &Final) at ~(300°C,90 bar)

x1 & x1.27

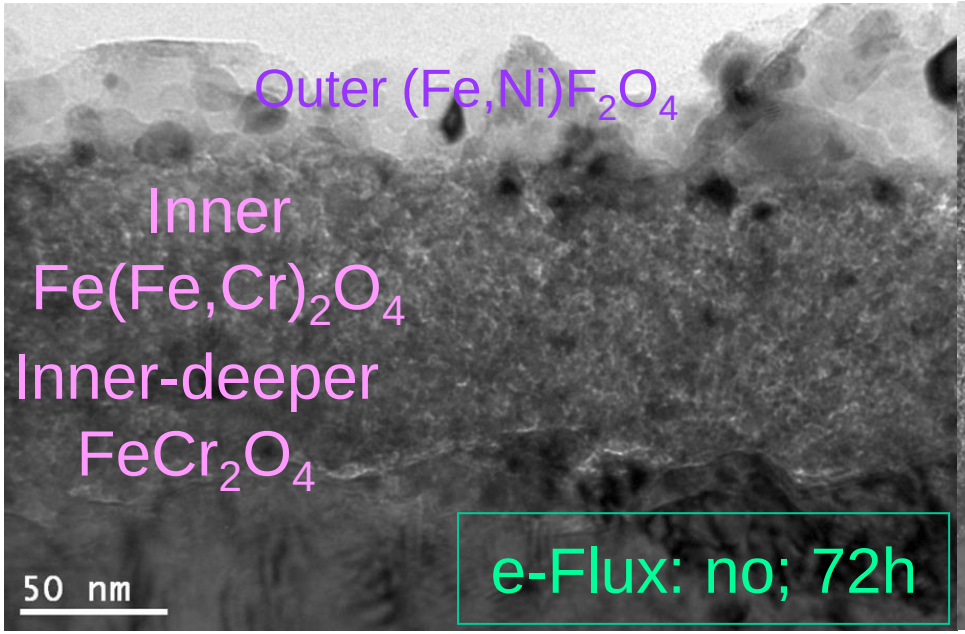

x1 & x1.27

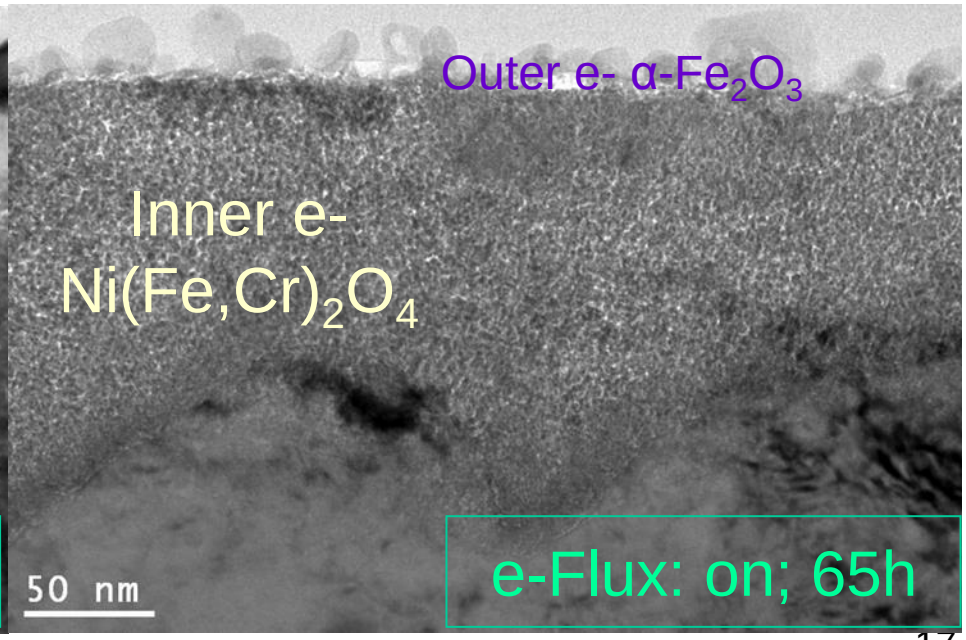

Depth~(< 0.1-0.4 μm)–Oxide layer after e- flux

Inner-layer (dense) : Fe(III)-enriched nickel chromite, $Ni(Fe,Cr)_2O_4$

outer-layer (dispersed crystallites (<50nm)): Fe(III) hematite α-Fe_2O_3

Inner-layer destruction: low density distribution of cavity (~(0.2-5) μm^2, depth (1-1.5μm), ~(1-5)x10^{-9} cm^{-2}

[cH_2](Initial) (Flux on/no flux): 3

Effect of e- flux on Oxide Growth at ~(300°C,90 bar) 316L(e-)/water(PWR,e-) interface (no flow rate)

Irradiation defects & Radiolysis Species Summary

e- Flux on: cavities (low density)

inner oxide destruction and dissolution

e- Flux on: composition change

Inner oxide: $Ni(Fe,Cr)_2O_4$

Ni(II) gain; Fe(II) loss

Outer oxide (crystallites): α-Fe_2O_3

Fe(III) gain; Ni(II) & Fe(II) loss

e- Flux on: release rate increase

rFe>>rNi> rCr (r: ratio of release rate: flux on vs flux no)

M.Wang 2013 Ph-D

Why Fe(III) enrichment and loss of Fe (II) ?

It seems to be consistent with the statement * that Fenton reactions Fe^{n+} with radolytic H_2O_2: peroxide favoring high ion valence state (*Barbusinki 2009)

PWR coolant circuit : confined zones

Merci pour votre attention

Fondation européenne
pour les énergies de demain
INSTITUT DE FRANCE